

Lawrence Berkeley National Laboratory

LBL Publications

Title

Dilution destabilizes engineered ligand-coated nanoparticles in aqueous suspensions

Permalink

<https://escholarship.org/uc/item/2pb8n34j>

Journal

Environmental Toxicology and Chemistry, 37(5)

ISSN

0730-7268

Authors

Wan, Jiamin
Kim, Yongman
Mulvihill, Martin J
et al.

Publication Date

2018-01-25

DOI

10.1002/etc.4103

Peer reviewed

Environmental Chemistry

Dilution Destabilizes Engineered Ligand-Coated Nanoparticles in Aqueous Suspensions

Jiamin Wan,^{a,*} Yongman Kim,^a Martin J. Mulvihill,^b and Tetsu K. Tokunaga^a^aEarth Sciences Division, Lawrence Berkeley National Laboratory, Berkeley, California, USA^bUC Berkeley Center for Green Chemistry, University of California, Berkeley, California, USA

Abstract: It is commonly true that a diluted colloidal suspension is more stable over time than a concentrated one because dilution reduces collision rates of the particles and therefore delays the formation of aggregates. However, this generalization does not apply for some engineered ligand-coated nanoparticles (NPs). We observed the opposite relationship between stability and concentration of NPs. We tested 4 different types of NPs: CdSe-11-mercaptopundecanoic acid, CdTe-polyelectrolytes, Ag-citrate, and Ag-polyvinylpyrrolidone. The results showed that dilution alone induced aggregation and subsequent sedimentation of the NPs that were originally monodispersed at very high concentrations. Increased dilution caused NPs to progressively become unstable in the suspensions. The extent of the dilution impact on the stability of NPs is different for different types of NPs. We hypothesize that the unavoidable decrease in free ligand concentration in the aqueous phase following dilution causes detachment of ligands from the suspended NP cores. The ligands attached to NP core surfaces must generally approach exchange equilibrium with free ligands in the aqueous phase; therefore, ligand detachment and destabilization are expected consequences of dilution. More studies are necessary to test this hypothesis. Because the stability of NPs determines their physicochemical and kinetic behavior including toxicity, dilution-induced instability needs to be understood to realistically predict the behavior of engineered ligand-coated NPs in aqueous systems. *Environ Toxicol Chem* 2018;37:1301–1308. © 2018 SETAC

Keywords: Dilution; Ligand-coated nanoparticle; Engineered nanoparticle; Aggregation; Silver nanoparticle; Cadmium selenide nanoparticle

INTRODUCTION

The rapid growth of nanotechnology has resulted in considerable economic development, yet its expanding use in many industries and products has raised considerable concerns over potential negative impacts of engineered nanoparticles (NPs) to human health and ecosystems (Biswas and Wu 2005; Bottero et al. 2015; Hardman 2006; Jiang et al. 2017; Lowry et al. 2012; Nel et al. 2006; Stankus et al. 2011; Wiesner et al. 2006). The surface properties of NPs determine their stability in water and consequently their long-range transport in aquatic environments and levels of uptake by organisms. Indeed, the chemistry of the aqueous phase, including natural organic matter (Jiang et al. 2017; Stankus et al. 2011), can strongly influence the fate of NPs in the environment. Therefore, understanding the stability of NPs in aquatic systems is an essential step for evaluating the risks they may pose when released into the environment (Brant et al. 2005;

Espinasse et al. 2007; Lecoanet et al. 2004; Owen and Handy 2007; Quevedo and Tufenkji 2009). The term “colloidal stability” in the present study is used to denote NP resistance to aggregation (flocculation), allowing their persistence as dispersed NP suspensions. Bare metal, metal-oxide, and semiconductor NPs do not remain suspended as monodispersed entities in aqueous solutions because their attractive van der Waals interactions overwhelm electrostatic repulsion, resulting in aggregation. However, coating NPs with hydrophilic ligands can prevent their aggregation. Commonly employed surface coatings for NPs include polymers, polyelectrolytes, and surfactants. Nanoparticle core-ligand binding mechanisms involve the same interactions as complexation of metal ions, including electrostatic attraction between ions, donor–acceptor interactions, and covalent bonding (Dabbousi et al. 1997). The coating covering the inorganic core determines NP surface properties and, therefore, its stability in aqueous suspensions. Nanoparticle coatings are designed and manufactured for different purposes, to stabilize NPs in desired fluids or to carry certain functional chemicals to the target locations. The science and technology of ligand coating enables exciting current and potential applications

* Address correspondence to jwan@lbl.gov

Published online 25 January 2018 in Wiley Online Library (wileyonlinelibrary.com).

DOI: 10.1002/etc.4103

of NPs. For instance, quantum dots, semiconductor nanocrystals with unique optical and transport properties, are useful in electronics, solar energy conversion, and biomedical imaging and will potentially be used for ultrahigh-density data storage and quantum information processing (Bruchez et al. 1998). Cadmium selenide (CdSe) and cadmium telluride (CdTe) are among the most useful quantum dots because their unique nanoscale optical and electronic properties make them excellent candidates for commercial applications. The hydrophobic metalloid crystalline core of quantum dots can be ligated with terminal functional groups to permit their stability in aqueous suspensions. The stability and mobility of quantum dot NPs in the environment are of growing concern because Cd and Se are toxic (Dumas et al. 2010; Lewinski et al. 2010; Quevedo and Tufenkji 2009; Zhang et al. 2008). It has been reported that photooxidation of the ligand-coated quantum dots is responsible for the high cytotoxicity of the quantum dot (Cho et al. 2007; Hoshino et al. 2004; Ma et al. 2006; Metz et al. 2009), and the stability of quantum dots protected by their coatings is the key to controlling their cytotoxicity (Lewinski et al. 2008). The success of some quantum dot technologies largely depends on the ability of the organic coatings to protect the inorganic cores from the solution environment. Therefore, quantum dot surface coatings should also be central for determining the environmental impacts of these substances in various use and disposal scenarios (Dabbousi et al. 1997). Recent studies on the environmental impacts of engineered NPs have been largely focused on silver (Ag) NPs because of their widespread applications in commercial products and potential high toxicity to the biosphere (Levard et al. 2012). These studies examined the stability, transport, solubility, and toxicity of engineered AgNPs (Bone et al. 2012; Kent and Vikesland 2012; Reinsch et al. 2012; Tejamaya et al. 2012; Tripathi et al. 2012; Unrine et al. 2012).

Experiments conducted in laboratories to understand NP behavior in natural environments utilize dilutions from highly concentrated stock suspensions that are commercially available or synthesized in the laboratory (Jana et al. 2015; Park et al. 2015). To obtain optimal analytical instrument responses, relatively high concentrations are often used. Concentrations of NPs in natural aquatic environments can vary by many orders of magnitude depending on the source and release process, but they invariably become more dilute on mixing with NP-free solutions. The conventional perception is that less concentrated NP suspensions are more stable because dilution increases diffusion distances and decreases collision frequency among the Brownian particles. However, guided by our own laboratory observations that NP suspensions became less stable on dilution, we decided to systematically test the dilution effect. We used 4 types of NPs: CdSe cores coated by 11-mercaptopundecanoic acid (CdSe-MUA), CdTe-polyacrylate, Ag-citrate (CIT), and Ag-polyvinylpyrrolidone (PVP). Because of limitations encountered in using conventional instrumentation such as dynamic light scattering (DLS) for measuring hydrodynamic particle/aggregate sizes and zeta potentials in diluted suspensions, we developed alternative methods to determine changes in size distributions.

MATERIALS AND METHODS

NPs

Four types of NPs were used in the present study, with 3 of them purchased and CdSe-MUA-NPs synthesized by a nanomaterial scientist at the Molecular Foundry of Lawrence Berkeley National Laboratory (Berkeley, CA, USA). The CdSeNPs were synthesized using CdO and trioctylphosphine selenide precursors in a mixture of oleylamine, oleic acid, and octadecene. The synthesis was done in a Symyx automated nanocrystal synthesizer using previously reported procedures (Chan et al. 2010; Mulvihill et al. 2010). The resultant CdSeNP cores are 4.4 ± 0.2 nm in diameter (measured using transmission electron microscopy [TEM]), capped with MUA ($\text{HS}[\text{CH}_2]_{10}\text{COOH}$) to make the particles hydrophilic. The thiol group of MUA binds to the CdSe core, thereby capping the NPs with exposed carboxyl groups. This resulted in the particles being negatively charged in typical environmental pH conditions (pK_a of the carboxylic acid is 3.7). The stock suspension had pH 10.3 and contained 88.3 ± 0.4 mM Cd, 85.6 ± 0.3 mM Se, and 3.0 mM Na^+ (measured by inductively coupled plasma mass spectrometry [ICP-MS] after dissolution in acid). The slightly lower than unity Se to Cd molar ratio ($\text{Cd:Se} = 1.0:0.97$) was reproducible through repeated measurements and may have been caused by volatile H_2Se loss during sample acidification for analysis. The average hydrodynamic diameter (D_h) of monodispersed MUA-coated CdSeNPs in the stock suspension is 8.0 ± 0.3 nm measured by DLS in 10 times diluted suspensions, in contrast to the 4.4 nm core size. The difference between the DLS-measured D_h value of 8.0 nm for ligand-coated NPs and the TEM-measured 4.4 nm for bare CdSe cores is consistent with a hydrated ligand shell, with the MUA length in the range of 1.5 nm. The concentrated stock suspension was stored in the dark in a refrigerator for the entire experiment duration (~ 6 mo). During this time the stock CdSe quantum dot suspensions remained dispersed.

The CdTe-polyacrylate-NPs used were purchased from Vive Nano (product no. 18010L). This stock suspension is described by the manufacturer as a 20 mg mL^{-1} aqueous suspension of 1- to 10-nm CdS-capped CdTeNPs, stabilized by Na-polyacrylate. Our measurements of the stock suspension (by ICP-MS) yielded 17.6 ± 0.3 mM Cd and only 2.4 ± 0.1 mM Te, pH 8.3. The core size was approximately 8 nm measured using TEM. However, the D_h was measured as 60.0 ± 23.3 nm by DLS at 10 times dilution. Both Ag-PVP and Ag-CIT were purchased from NanoComposix. Based on the manufacturer's information, the Ag-PVP (lot no. JME1104) stock suspension contains 1 mg Ag/mL and 2.1×10^{14} particles/mL, with a core size of 9.5 ± 1.7 nm (TEM). Our measurements indicated an average $D_h = 30.2 \pm 0.3$ nm at 10 times dilution and pH 6.9. The Ag-CIT (lot no. KJW 1012) stock suspension contains 1 mg Ag/mL and 2.1×10^{14} particles/mL, with a core size 9.6 ± 1.3 nm (TEM). At 10 times dilution, our measures yielded average $D_h = 15.3 \pm 0.5$ nm and pH 6.1.

Making NP dilutions

The dilution factors (e.g., 100 times . . . 1000 times) used in the present study refer to dilutions from the original synthesized or

purchased concentrated NP stock suspensions. Nanoparticle dilutions were prepared with nanopure water. All experiments were conducted at room temperature ($23 \pm 0.5^\circ\text{C}$). To make diluted suspensions from a stock suspension, a common background solution containing 1.0 mM NaCl with pH 9.0 (for CdSeNPs and CdTeNPs) and 6.5 (for AgNPs; adjusted using NaOH and HCl) was first prepared. The pH and ionic strength were chosen to be close to the pH of the stock solutions. In making each dilution, a calculated volume of a stock suspension was mixed with the background solution. This resulted in all suspensions having different dilution factors, a common pH of approximately 9.0 or 6.5, and ionic strength of approximately 1.0 mM NaCl. Directly adding droplets of acid or base to suspensions to adjust pH was avoided because this would induce local irreversible aggregation. Stock suspensions were diluted with a range of dilution factors from 10 to 1000 times.

Using DLS to measure NP dynamic size

The commonly used method for determining sizes and zeta potentials of NPs is DLS (Lewinski et al. 2008). We used a DLS instrument (ZetaPlus; Brookhaven) to measure D_h and zeta potentials as functions of dilution factors. Each dilution was made fresh, just before conducting the DLS measurement. To keep the time between dilution and the initiation of data collection constant, each dilution was performed and measured individually. The D_h data collections were initiated within 3 min of the actual dilutions. The D_h data were collected at 30-s intervals for 50 min. A duplicate sample for each dilution was prepared for zeta potential measurement using the same DLS instrument.

Using filtration method for NP dynamic size

To circumvent limitations of indirect size measurements that are unable to handle dilute polydisperse suspensions, we employed a filtration size fractionation method to determine sizes of the NPs as functions of dilution factor and time. Nanoparticles of CdSe-MUA and Ag-CIT were selected for this experiment. For each of these NP types, 5 dilutions were made from their stock suspensions (10 mL each in a vial) with duplicates. These 5 suspensions were statically stored in the dark and mixed only at the sampling times for obtaining representative samples. Subsamples were taken from each vial at 3 times: 0, 5, and 10 d. The “day 0” samples were taken and filtered approximately 1 h after the dilutions were made. At each sampling time, 4 subsamples (0.5 mL each) from each vial were taken after mixing. Three of the 4 subsamples were filtered through 3 different-sized filters (inorganic membranes, Anotop Syringe Filters; Whatman): 20, 100, and 200 nm, respectively. The remaining unfiltered subsample was used for determining the baseline concentrations. All filtered suspensions together with the unfiltered baseline sample were acid-digested and then analyzed for Cd or Ag concentrations (ICP-MS). Data from each filtered subsample were normalized by their baseline (bulk suspension) concentration, resulting in size fraction distributions as functions of dilution factor and time.

Visualization of sedimentation time versus dilution factor

We selected CdSe-MUA to conduct this experiment because its intense color yielded good photographic images, even in highly diluted suspensions. This experiment involved allowing CdSeNPs to sediment by gravity in suspensions of different dilutions, with daily photographic image acquisition. To shorten the time required for NP sedimentation to a reasonable image-recording time frame, the suspensions were made in 100 mM NaCl solution, pH 9.0. Note that this was the only experiment conducted at 100 mM NaCl. The stock CdSeNP suspension was diluted with a solution of 100 mM NaCl (pH 9) by factors of 10, 100, 200, 400, and 800 times; and each dilution was transferred into a conical centrifuge tube. The sealed centrifuge tubes were stored under a dark cover during the experiment to minimize light exposure and uncovered on a daily basis only when a photograph was taken.

RESULTS AND DISCUSSION

Dynamic sizes measured using DLS

The most commonly used commercially available instrument for determining hydrodynamic diameters (D_h) of NPs and their aggregates in suspensions is DLS. It is necessary to first understand how the DLS measurements of D_h varied as a function of NP dilution. The DLS-measured D_h values of 4 different types of NPs in suspensions with different dilution factors are presented in Figure 1. Within the experimental time duration of 50 min the results did not show interpretable trends in D_h values (starting times were ≤ 5 min after actual dilutions). Instead, the D_h values became progressively divergent with increased dilution. In the 10 times dilutions, CdSe, Ag-CIT, and Ag-PVP were monodispersed with a unique average D_h value of 8.0 ± 0.3 , 30.2 ± 0.5 , and 15.3 ± 0.3 nm, respectively. The CdTeNPs have an average D_h value of 60 ± 23.3 nm, suggesting that the CdTeNPs were not as monodispersed in the 10 times suspension as the other tested NPs. The CdTeNP suspensions degraded the most with progressive dilution, with the majority of the particles measured by DLS being apparently larger than 1000 nm even at 100 times dilution. The CdSeNPs and Ag-CIT-NPs showed similar trends, with reasonably consistent D_h values up to 100 times dilution but not beyond 300 and 400 times dilutions. The Ag-PVP-NPs were more stable compared to the other 3 types, although it also exhibits decreased stability with increased dilution.

It is important to recognize limitations of using DLS in measurements of dilute, polydisperse suspensions (Mulvihill et al. 2010). The DLS instrument is well suited for characterization of NP monodispersions, but the obtained sizes in complex polydispersions are approximations with potentially high uncertainties. This is especially true when the polydispersed NPs are suspended in mixtures with detached ligands and their aggregates. The results in Figure 1 clearly demonstrate that the DLS instrument became less suitable for NP suspensions with increased dilution. Nevertheless, the results suggest that the extents of destabilization and aggregation are different

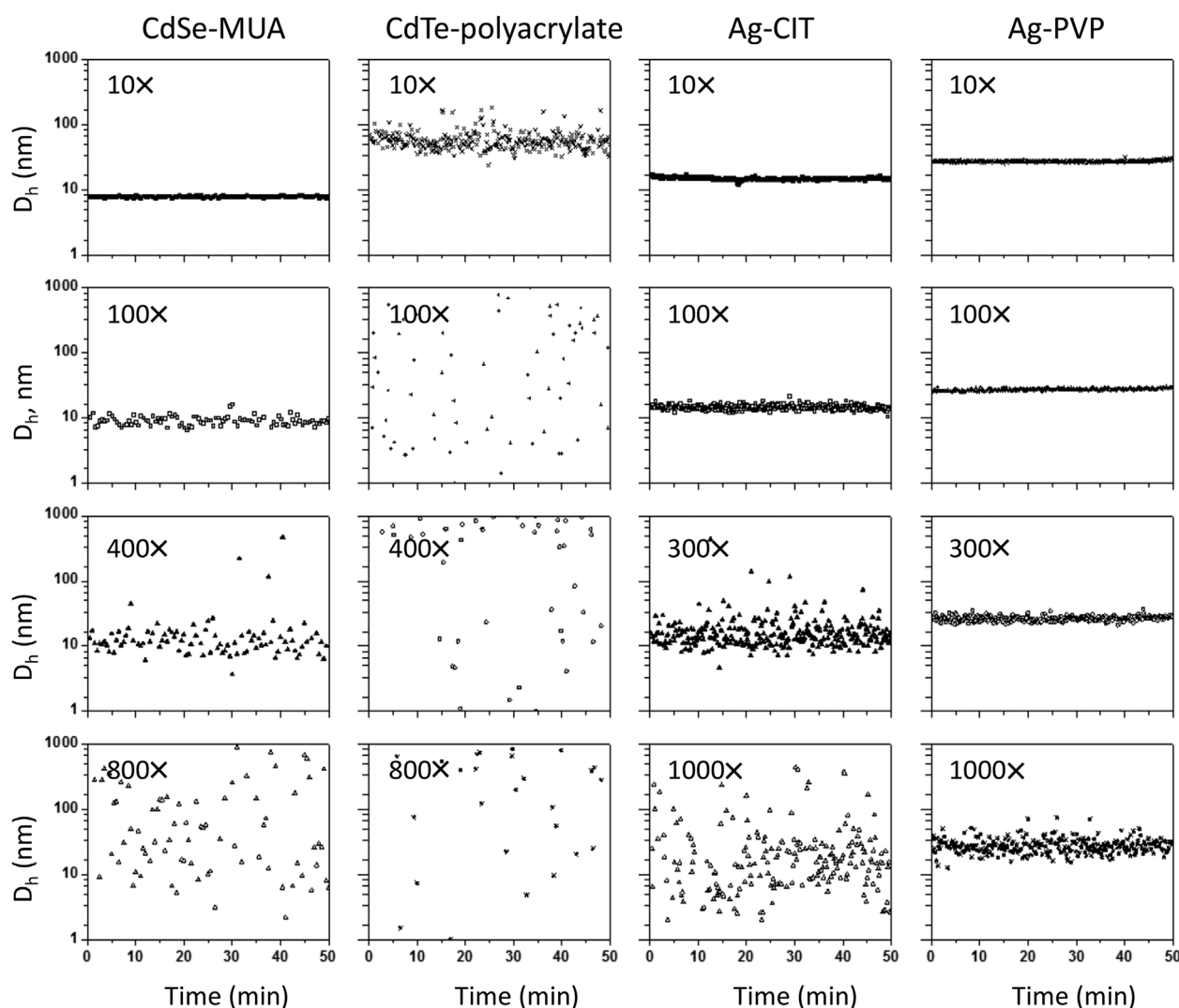


FIGURE 1: Measured nanoparticle (NP) hydrodynamic diameters (D_h) in suspensions with different dilution factors, using dynamic light scattering. Four different types of NPs were measured. All suspensions contained 1.0 mM NaCl, and pH values were close to that of their original stock suspensions. Results show that the measured D_h values are more scattered with greater dilution of NP suspensions. Ag-CIT = silver citrate; Ag-PVP = silver polyvinylpyrrolidone; CdSe-MUA = cadmium selenide-11-mercaptopundecanoic acid; CdTe = cadmium telluride.

for different types of NPs depending on the nature of the coatings.

In principle, the zeta potential provides an estimate of charge density of particle surfaces, with higher magnitudes indicative of higher charge density. If ligand dissociation occurs as a result of dilution, the magnitude of the zeta potentials should decrease as the dilution factor is increased. Our measured zeta potentials showed a trend of decreased magnitude (becoming less negative) with increased dilution up to 100 times but were not reproducible for dilutions beyond 100 times (data not shown). Given the common use of DLS in zeta-potential and D_h measurements, it is worth noting that use of this method can be problematic when particles become polydisperse as dilution is increased. The lack of reproducibility in measured zeta potentials, especially for suspensions with higher dilution factors, showed that the DLS method is not suitable for determining zeta potentials in diluted suspensions, and these measurements are not reported in the present study.

Time-dependent size fractions determined by filtration

Filtration of NP suspensions through sets of different pore-size filters fractionates NP suspensions into discrete size ranges and allows detection of any dilution- and time-dependent changes in size distributions. The filtration-determined dynamic size fractions for 5 different dilutions (from 10 to 1000 times) of CdSe-MUA and Ag-CIT on different days are presented in Figures 2 and 3, respectively. The figures present the measured mass percentages of Cd or Ag in 4 different size fractions separated through filters of 3 different sizes: 20, 100, and 200 nm (3 parallel suspensions were used, each for a different filter size, and the Cd/Ag concentration in each solution was determined with ICP-MS). On the graphs the data of <20-nm fractions were directly measured. The 20- to 100-nm fraction masses were calculated by subtracting the measured <20-nm masses from the measured <100-nm masses, the 100- to 200-nm masses

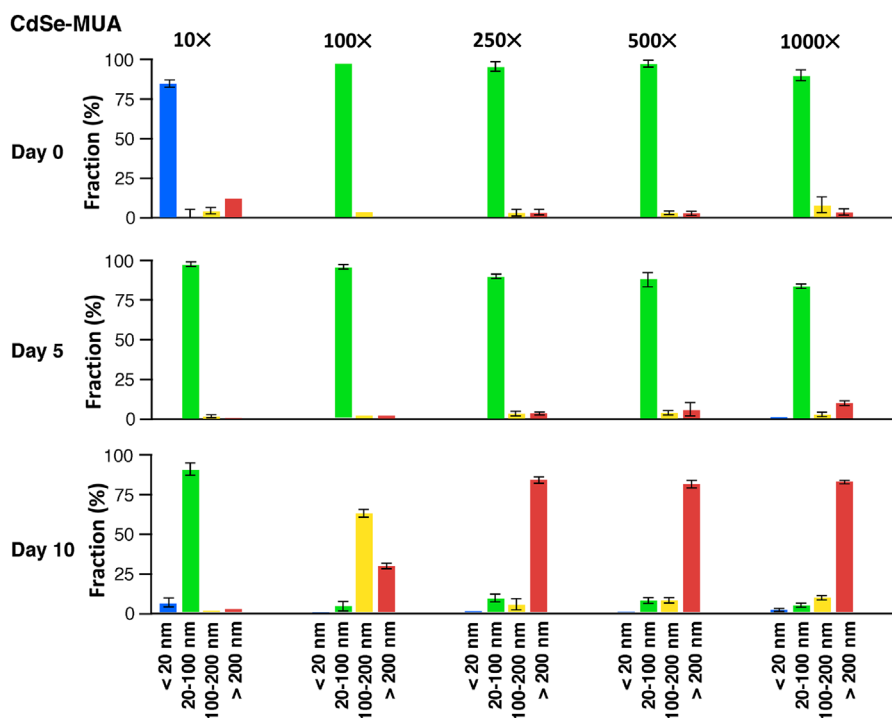


FIGURE 2: Time-dependent size fractions of cadmium selenide-11-mercaptopundecanoic acid nanoparticles/aggregates determined by filtration in 5 different dilutions. All suspensions contained 1.0 mM NaCl and had pH 9.0. Samples were fractionated through filters on days 0, 5, and 10. Filtered and bulk (baseline) suspensions were acid-digested and analyzed using inductively coupled plasma mass spectrometry for Cd concentrations. Data from each filtered subsample were normalized by the baseline concentration, resulting in size fraction distributions as functions of dilution factor and time. Range bars indicate the lower and higher values from duplicate samples. CdSe-MUA = cadmium selenide-11-mercaptopundecanoic acid.

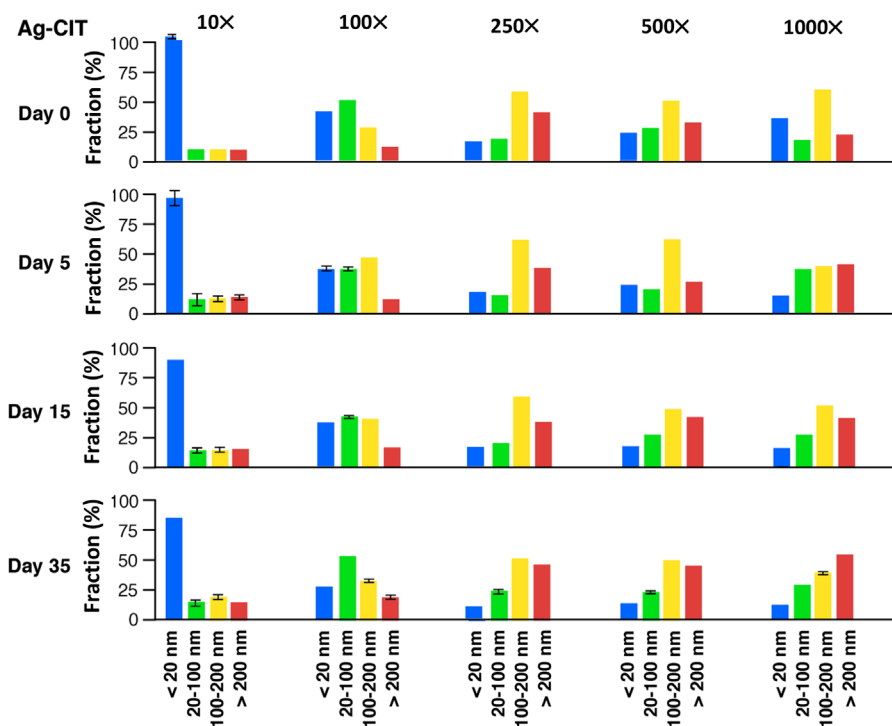


FIGURE 3: Time-dependent size fractions of silver citrate nanoparticles/aggregates determined by filtration in 5 different dilutions. All suspensions contained 1.0 mM NaCl and had pH 6.5. Samples were fractionated through filters on days 0, 5, 15, and 35. Filtered and bulk (baseline) suspensions were acid-digested and analyzed for Ag concentrations by inductively coupled plasma mass spectrometry. Range bars indicate the lower and higher values from duplicate samples. Ag-CIT = silver citrate.

were calculated by subtracting the <100-nm masses from the <200-nm masses, and the >200-nm masses were obtained by subtracting the <200-nm masses from the baseline (total concentrations) values. The average values of duplicate samples are shown in the figures. For the day 0 data, the suspensions were filtered within 1 h after the dilutions.

Aggregation of CdSeNPs occurred in all dilutions, even on day 0 (Figure 2). On day 0, for the lowest dilution (10 times), >80% of NPs are measured in the finest fraction of <20 nm. However, at higher dilutions, NPs were completely converted to the next size category, 20- to 100-nm clusters, within a few hours (for all ≥ 100 times dilutions). Two parameters determine the rate and extent of aggregation: collision frequency and attachment efficiency of the NPs (Levard et al. 2012). Collision frequency is determined by the distance between 2 nearby suspended particles (the concentration) and particle size and mass. The collision efficiency represents the fraction of collisions that result in aggregation, controlled by the NP surface stickiness. If the NP surfaces maintained the same collision efficiency in the different dilutions, the decreased collision frequency from increased dilution would have decreased the aggregation rate. Reduced NP surface charge density from detachment of ligand coatings following dilution would diminish interparticle repulsion and increase collision efficiency. In addition, decreased steric hindrance may play a role for particles with polymer coatings such as PVP. The fact that the aggregation rates generally increased with dilution indicates that collision efficiencies increased more than enough to counterbalance the decreased collision frequencies. The time required for growth of CdSeNPs from predominantly 20- to 100-nm to >200-nm aggregates took 5 to 10 d for the 100, 250, 500, and 1000 times dilutions, with

aggregation in the 100 times dilution lagging slightly behind at day 10. The 10 times dilution was the most stable suspension, taking up to 5 d to complete the early-stage aggregation (collisions of primary NPs within the shortest distance), and showed no significant further growth by day 10. This observed time sequence clearly demonstrates that collision efficiencies of the NPs increased as the dilutions increased. Dilution indeed decreased the colloidal stability (increased aggregation) of suspended CdSeNPs, and the higher the dilution was, the less stable the NPs in suspensions.

The same experiment was conducted on Ag-CIT-NPs, and their filtration size fraction data are presented in Figure 3. The same conclusions obtained from the CdSeNPs are supported by the Ag-CIT-NP results, with the only differences found in the overall aggregation rates promoted by dilution. The day 0 data exhibited aggregation in all dilutions ≥ 100 times, with a larger extent in ≥ 250 times dilutions, similar to the CdSeNPs. Although the size fraction distributions for the 250, 500, and 1000 times dilutions have no large differences, considering the much increased distance between the adjacent NPs as the dilution increased (decreased collision frequency), the data suggest that the higher dilution corresponded to the high collision efficiency. The aggregate sizes showed progressive growth with time, most clearly demonstrated in 1000 times dilutions and even for the most stable (the least diluted, 10 times dilution). The rates of dilution-induced aggregation are slower for Ag-CIT than for CdSe-MUA. The only possible explanation for the decreased stability following dilution is that the NPs lose their charged ligand coatings on dilution. Dilution reduced the free ligand concentration in solution, which drives detachment of ligands from NP surfaces.

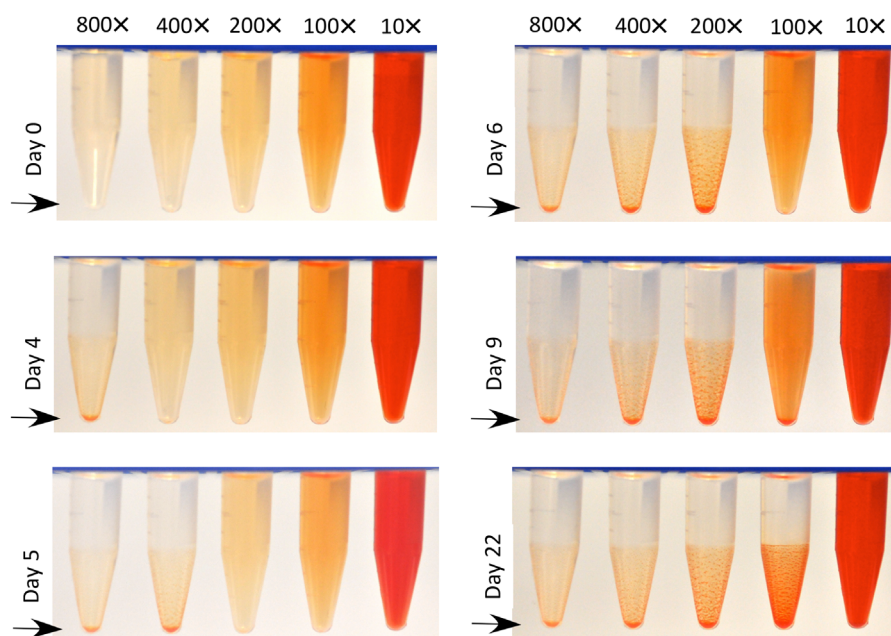


FIGURE 4: Photographs showing sedimentation of nanoparticles (NPs) of cadmium selenide-11-mercaptoundecanoic acid as a function of dilution. All solutions contained 100 mM NaCl at pH 9.0. Over time, the originally suspended NPs formed aggregates and sedimented to the bottoms of the vials. Sedimentation occurred progressively earlier in more diluted suspensions, demonstrating that dilution caused destabilization of NP suspension. CdSe-MUA = cadmium selenide cores coated by 11-mercaptoundecanoic acid.

Visual observations of dilution-dependent NP sedimentation

To further test our hypothesis, we used an additional method of monitoring NP sedimentation following aggregation. Five dilutions of the CdSe-MUA-NPs were tested: 800, 400, 200, 100, and 10 times. Photographs of these NP suspensions obtained on selected days are shown in Figure 4. On day 0, all NPs were uniformly suspended in water (evident from optical uniformity within each tube). Sedimentation first was observed on day 4 in the most diluted (800 times) suspension, followed on day 5 in 400 times dilution, on day 6 in 200 times dilution, then on day 9 in 100 times dilution. On day 22 the NPs still appear to remain suspended in the 10 times dilution. If the surface charge properties of the NPs remained unchanged (equal collision efficiency) in all 5 dilutions, the sedimentation time sequence should have been reversed because of the higher collision frequency in less dilute suspensions. This simple experiment unambiguously demonstrated that dilution caused NP destabilization, resulting in more rapid NP aggregation and sedimentation.

Environmental implications

Some engineered ligand-coated NPs will inevitably find their way into aquatic environments, soils, and sediments. Depending on the source and nature of release, their concentrations in environmental waters vary greatly but most likely are low at any significant distance away from the discharge point. Inevitable decreases in free-ligand concentrations on NP entry into environmental waters may drive ligand (including polymers, polyelectrolytes, and surfactants) detachment, resulting in NPs becoming less charged. The reduced surface charge density of NPs may promote their aggregation, as well as their stronger sorption to soil and sediment matrix surfaces. Therefore, these engineered, ligand-coated NPs are expected to be much less mobile in the natural environment than in laboratory tests conducted on highly concentrated suspensions. This finding also has relevance in other applications where the ligand-coated NPs are used for different purposes. The dilution of initially highly concentrated and stable NP suspensions by mixing with water may cause detachment of ligand coatings and alter the originally designed surface properties. Therefore, predictions of NP mobility in the environment based on laboratory experiments conducted with very high NP concentrations are not reliable. Understanding the dilution effect on NP suspension stability is necessary for reliably predicting the fate and transport of engineered NPs.

Acknowledgment—The present study was conducted as part of the Scientific Focus Area at Lawrence Berkeley National Laboratory funded by the US Department of Energy (DOE) Subsurface Biogeochemical Research Program, DOE Office of Science, Office of Biological and Environmental Research, under Contract Number DE-AC02-05CH11231. We thank the anonymous reviewers for their helpful comments.

Data Availability—Data, associated metadata, and calculation tools are available from the corresponding author (jwan@lbl.gov).

REFERENCES

- Biswas P, Wu CY. 2005. Nanoparticles and the environment. *J Air Waste Manag Assoc* 55:708–746.
- Bone AJ, Colman BP, Gondikas AP, Newton KM, Harrold KH, Cory RM, Unrine JM, Klaine SJ, Matson CW, Di Giulio RT. 2012. Biotic and abiotic interactions in aquatic microcosms determine fate and toxicity of Ag nanoparticles: Part 2—Toxicity and Ag speciation. *Environ Sci Technol* 46:6925–6933.
- Bottero JY, Auffan M, Borschnek D, Chaurand P, Labille J, Levard C, Masion A, Tella M, Rose J, Wiesner MR. 2015. Nanotechnology, global development in the frame of environmental risk forecasting. A necessity of interdisciplinary researches. *Comptes Rendus Geoscience* 347:35–42.
- Brant J, Lecoanet H, Wiesner MR. 2005. Aggregation and deposition characteristics of fullerene nanoparticles in aqueous systems. *J Nanopart Res* 7:545–553.
- Bruchez MJ, Moronne M, Gin P, Weiss S, Alivisatos AP. 1998. Semiconductor nanocrystals as fluorescent biological labels. *Science* 281:2013–2016.
- Chan EM, Xu C, Mao AW, Han G, Owen JS, Cohen BE, Milliron DJ. 2010. Reproducible, high-throughput synthesis of colloidal nanocrystals for optimization in multidimensional parameter space. *Nano Lett* 10:1874–1885.
- Cho SJ, Maysinger D, Jain M, Roder B, Hackbarth S, Winnik FM. 2007. Long-term exposure to CdTe quantum dots causes functional impairments in live cells. *Langmuir* 23:1974–1980.
- Dabbousi BO, RodriguezViejo J, Mikulec FV, Heine JR, Mattoussi H, Ober R. 1997. CdSe/ZnS core-shell quantum dots: Synthesis and characterization of a size series of highly luminescent nanocrystallites. *J Phys Chem B* 4:9463–9475.
- Dumas E, Gao C, Suffern D, Bradforth SE, Dimitrijevic NM, Nadeau JL. 2010. Interfacial charge transfer between CdTe quantum dots and gram negative vs gram positive bacteria. *Environ Sci Technol* 44:1464–1470.
- Espinasse B, Hotze EM, Wiesner MR. 2007. Transport and retention of colloidal aggregates of C60 in porous media: Effects of organic macromolecules, ionic composition and preparation method. *Environ Sci Technol* 41:7396–7402.
- Hardman R. 2006. A toxicologic review of quantum dots: Toxicity depends on physicochemical and environmental factors. *Environ Health Perspect* 114:165–172.
- Hoshino A, Fujioka K, Oku T, Suga M, Sasaki Y, Ohta T. 2004. Physicochemical properties and cellular toxicity of nanocrystal quantum dots depend on their surface modification. *Nano Lett* 11:2163–2169.
- Jana S, Phan TNT, Bouet C, Tessier MD, Davidson P, Dubertret B, Abecassis B. 2015. Stacking and colloidal stability of CdSe nanoplatelets. *Langmuir* 31:10532–10539.
- Jiang CJ, Castellon BT, Matson CW, Aiken GR, Hsu-Kim H. 2017. Relative contributions of copper oxide nanoparticles and dissolved copper to Cu uptake kinetics of gulf killifish (*Fundulus grandis*) embryos. *Environ Sci Technol* 51:1395–1404.
- Kent RD, Vikesland PJ. 2012. Controlled evaluation of silver nanoparticle dissolution using atomic force microscopy. *Environ Sci Technol* 46:6977–6984.
- Lecoanet HFB, Bottero JY, Wiesner MR. 2004. Laboratory assessment of the mobility of nanomaterials in porous media. *Environ Sci Technol* 38:545–553.
- Levard C, Hotze EM, Lowry GV, Brown GE. 2012. Environmental transformations of silver nanoparticles: Impact on stability and toxicity. *Environ Sci Technol* 46:6900–6914.
- Lewinski N, Colvin V, Drezek R. 2008. Cytotoxicity of nanoparticles. *Small* 4:26–49.
- Lewinski NA, Zhu HG, Jo HJ, Pham D, Kamath RR, Ouyang CR, Vulpe CD, Colvin VL, Drezek RA. 2010. Quantification of water solubilized CdSe/ZnS quantum dots in *Daphnia magna*. *Environ Sci Technol* 44:1841–1846.
- Lowry GV, Gregory KB, Apte SC, Lead JR. 2012. Transformations of nanomaterials in the environment. *Environ Sci Technol* 46:6893–6899.
- Ma J, Chen J-Y, Guo J, Wang CC, Yang WL, Xu L, Wang PN. 2006. Photostability of thiol-capped CdTe quantum dots in living cells: The effect of photo-oxidation. *Nanotechnology* 17:2083–2089.
- Metz KM, Mangham AN, Bierman MJ, Jin S, Hamers RJ, Pedersen JA. 2009. Engineered nanomaterial transformation under oxidative environmental

- conditions: Development of an in vitro biomimetic assay. *Environ Sci Technol* 43:1598–1604.
- Mulvihill MJ, Habas SE, Plante IJ, Wan J, Mokari M. 2010. Influence of size, shape, and surface coating on the stability of aqueous suspensions of CdSe nanoparticles. *Chem Mater* 22:5251–5257.
- Nel A, Xia T, Madler L, Li N. 2006. Toxic potential of materials at the nanolevel. *Science* 311:622–627.
- Owen R, Handy R. 2007. Formulating the problems for environmental risk assessment of nanomaterials. *Environ Sci Technol* 41:5582–5588.
- Park SY, Kim HS, Yoo J, Kwon S, Shin TJ, Kim K, Jeong S, Seo YS. 2015. Long-term stability of CdSe/CdZnS quantum dot encapsulated in a multi-lamellar microcapsule. *Nanotechnology* 26:275602.
- Quevedo IR, Tufenkji N. 2009. Influence of solution chemistry on the deposition and detachment kinetics of a CdTe quantum dot examined using a quartz crystal microbalance. *Environ Sci Technol* 43:3176–3182.
- Reinsch BC, Levard C, Li Z, Ma R, Wise A, Gregory KB, Brown GE, Lowry GV. 2012. Sulfidation of silver nanoparticles decreases *Escherichia coli* growth inhibition. *Environ Sci Technol* 46:6992–7000.
- Stankus DP, Lohse SE, Hutchison JE, Nason JA. 2011. Interactions between natural organic matter and gold nanoparticles stabilized with different organic capping agents. *Environ Sci Technol* 45:3238–3244.
- Tejamaya M, Romer I, Merrifield RC, Lead JR. 2012. Stability of citrate, PVP, and PEG coated silver nanoparticles in ecotoxicology media. *Environ Sci Technol* 46:7011–7017.
- Tripathi S, Champagne D, Tufenkji N. 2012. Transport behavior of selected nanoparticles with different surface coatings in granular porous media coated with *Pseudomonas aeruginosa* biofilm. *Environ Sci Technol* 46:6942–6949.
- Unrine JM, Colman BP, Bone AJ, Gondikas AP, Matson CW. 2012. Biotic and abiotic interactions in aquatic microcosms determine fate and toxicity of Ag nanoparticles. Part 1. Aggregation and dissolution. *Environ Sci Technol* 46:6915–6924.
- Wiesner MR, Lowry GV, Alvarez PJJ, Dionysiou D, Biswas P. 2006. Assessing the risks of manufactured nanomaterials. *Environ Sci Technol* 40:4337–4445.
- Zhang Y, Chen YS, Westerhoff P, Crittenden JC. 2008. Stability and removal of water soluble CdTe quantum dots in water. *Environ Sci Technol* 42:321–325.